

Inverse Kinematic Synthesis of Motion Generation Four-bar Stamping Mechanism

Bilal M Oraik, Nurnadiah Zamri, Yahia M. Al-Smadi

Abstract: Stamping mechanism is found in different shapes and forms in the market. The stamping mechanism synthesis in this paper is unconventional Stamping mechanism where function/motion based synthesis have been presented using nonlinear optimization algorithm carried in matrix inversion or inverse kinematics and Newton Raphson numerical method. The Intended motion of the stamping mechanism will be achieved using four-bar motion generation that will go through or approximately the prescribed poses. Also the synthesized mechanism must satisfy the design variables mentioned herein; Grashof's condition should be incorporated in the optimization algorithm and should be satisfied. Another feature that should be incorporated to ascertain the functionality of the proposed work is the transmission angle (μ) which should be between 50° and 135° . Also the clearance for the stamping (stroke of the ram to bottom dead center (BDC)) should exceed 1 cm. The synthesized stamping machine was built in ADAMS to extract the trace path of the ram, transmission angle and driving crank angle. All results were within acceptable limits of the proposed conditions. The achieved mechanism motion passes through prescribed poses with very minimum error of 0.2% cm.

Index Terms: About four key words or phrases in alphabetical order, separated by commas.

I. INTRODUCTION

Press machines or mechanisms have been around since the birth of industrial revolution, they come in different shapes and sizes. However, once can categorize them as shown in Fig. 1 according to their uses and applications (i.e. the lower box group) and how many links in the mechanism (i.e. the upper box group). Many applications as examples comprises of either two jaws or one jaw pressing on an object to either form, dent or fix it. For example, plier mechanism is five bar pressing mechanism, spot welding is four bar pressing mechanism, orange juice maker is six bar mechanism and many more press mechanisms are out there covering wide spectrum of applications. Just to mention few mechanism shown in Fig. 2 a and b, also examples can be found in eight-bar spot welding mechanism [1], four –bar clamp mechanism [2], Five-bar

stamping mechanism [3] and eight-bar press mechanism [4]. Many researchers have studied press mechanisms; this paper will focus on the synthesis of four-bar stamping mechanism using motion generation as shown in Fig. 3. The fixed pivots a_0 and b_0 while the moving pivots a_1 and b_1 drive the links (i.e. crank $a_0 a_1$, follower $b_0 b_1$ and coupler $a_1 b_1$) to the desired motion or trajectory represents. The construction of the nonlinear optimization using matrix approach and inverse kinematics will minimize the structural error between the prescribed poses represented by the coupler points $p, q,$ and r and the synthesized (i.e. achieved) poses.

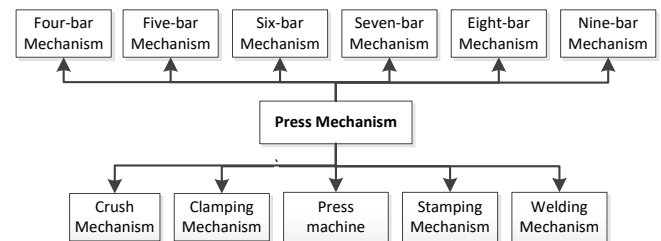


Figure 1: Categorization of press mechanism or linkage based on applications and number of links

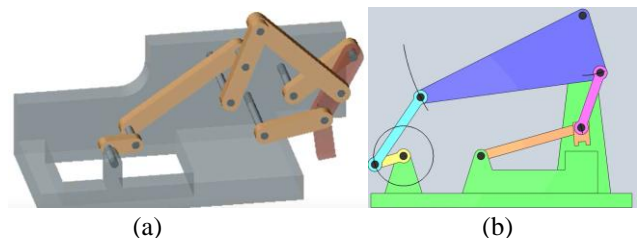


Figure 2: Press mechanisms, a) eight-bar mechanism [5] and b) six-bar press mechanism [6]

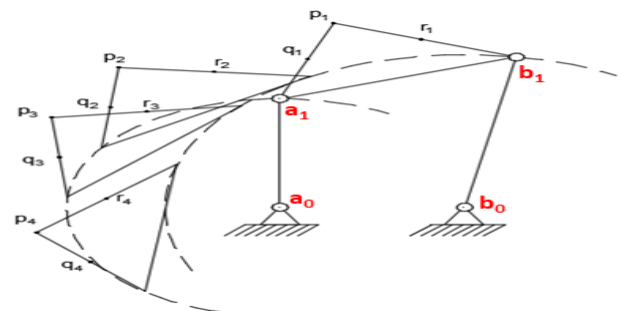


Figure 3: Prescribed rigid-body poses and calculated planar Four-Bar mechanism.

Researchers have studied, analyzed and synthesized these press mechanisms for different aspects using different approaches and trying to investigate certain issues relating to the motion of press mechanisms. Graphical presentation of stamping four bar mechanism has been introduced in [7] where three position graphical synthesis has been used also slider-crank four bar

Revised Manuscript Received on 30 May 2019.

* Correspondence Author

Bilal M. Oraik*, Faculty of Informatics and Computing, University Sultan Zainal Abidin, Besut Campus, 22200 Besut, Terengganu, Malaysia.

Nurnadiah Zamri, Faculty of Informatics and Computing, University Sultan Zainal Abidin, Besut Campus, 22200 Besut, Terengganu, Malaysia.

Yahia M. Al-Smadi, Department of Mechanical Engineering, Jordan University of Science and Technology, Irbid 22110, Jordan.

© The Authors. Published by Blue Eyes Intelligence Engineering and Sciences Publication (BEIESP). This is an open access article under the CC-BY-NC-ND license <http://creativecommons.org/licenses/by-nc-nd/4.0/>

Inverse Kinematic Synthesis of Motion Generation Four-bar Stamping Mechanism

mechanism of stamping mechanism is shown in [8]. Other mechanisms with more linkages were synthesized for press mechanisms, for example Watt-mechanism (six bar) [9] Stephenson mechanism (six-bar) [10] and [11] seven-bar press mechanism [12] and [13], eight-bar press mechanism as the one shown in Fig. 1 and nine-bar mechanism in [14]. most of these mechanisms rely on slider and crank configuration. researchers Graphical presentation of stamping four bar mechanism machine[7] also Vinogradov in his book [8] shows four-bar slider crank stamping machine. Watt-mechanism for press mechanism (six-bar)[9] Stephenson Mechanism (six bar) [10] and [11], vector approach for seven-bar press mechanism [12] and [13], eight-bar press mechanism as well as the one shown in Fig. 2 forward kinematics (FK) was used by all researchers in all kinds of press machines. FK is performed in the optimization synthesis technique in watt press press mechanism based on trajectory curve and crank input speed [9]. In [10], the optimization techniques was based on instant center analysis method and software ADAMS for comparative analysis to study the effect of design veraibales on several mechanisms. Dimensional synthesis with vector approach was used in [12] and [13] to investigate seven-bar press mechanism for deep drawing, with the emphasis on the position of bottom dead center (BDC) and working stroke length. Combining the linkage synthesis using vector approach and trial and error method in order to optimize the dimensions of the nin-bar press mechanism was used in [14] to study the influence of the ram position and BDC. Not only press or stamping machine was introduced using linkage mechanism. welding machine using Hoecken linkage (i.e. four-bar mechanism) [15] Clamping mechanism in [16] was actuated by the worm gear and the optimization process rely on the priciple of virtual work and the synthesis was performed using vector approach. This is unlike the work done in [17], where the mechanism is actuated by hydraulic cylinder and CAD approach was used too synthesizze the clamping mechanism, the synthesis used in [18] was performed in ADAMS for the five-bar pneumatically driven clamping mechanism. The clamping mechanism in [19] use position, velocity and acceleration analysis through using vector approach to synthesis the intended four-bar mechanism.

The rational of this research is to use matrix approach in order to design numerically four-bar stamping mechanism which then can be used in robotic application. we need to solve the mechanism assuming the end effector is moving in a certain motion, then take this motion and follow inverse kinematic approach to find out the closest location for moving hinges (\mathbf{a}_1 and \mathbf{b}_1) and fixed hinges (\mathbf{a}_0 and \mathbf{b}_0) in Fig. 3.

II. NUMERICALT RAJECTORY PLANING MATRICES BY DIRECT MATRIX INVERSION

A. Motion Modeling

Trajectory planning was optimized using genetic algorithm [20]. Minimum Jerk Path Generation with energy minimization for robot hand manipulator [21] and [22]. This work will present the mathematical formulation and derivation of mechanism synthesis based on Suh and Radcliff [23]. The basic rotation matrix equation as in (1) describes the

rotation of any vector fixed in a rigid body. The vector is conveniently described in terms of two points fixed in the body, a reference point \mathbf{p} at the tail of the vector, and a point of interest \mathbf{q} at the head of the vector. For plane rigid body motion (Fig. 4), the transformation (i.e. rotation and translation) of points \mathbf{p} and \mathbf{q} can be written as equation 1

$$\begin{bmatrix} q_x - p_x \\ q_y - p_y \end{bmatrix} = \begin{bmatrix} \cos \theta & -\sin \theta \\ \sin \theta & \cos \theta \end{bmatrix} \begin{bmatrix} q_{1x} - p_{1x} \\ q_{1y} - p_{1y} \end{bmatrix} \quad (1)$$

Where θ is the rotation of the rigid body with respect to a fixed set of x, y axes. Equation (1) may be written in the compact form

$$(\mathbf{q} - \mathbf{p}) = [R_\theta](\mathbf{q}_1 - \mathbf{p}_1) \quad (2)$$

Typically, the original position \mathbf{p}_1 and the final position \mathbf{p} for the reference point are given along with the rotation angle θ . Equation (2) can then be rearranged in a form suitable for calculation of the coordinates of the new position of point \mathbf{q} when its first position \mathbf{q}_1 is specified.

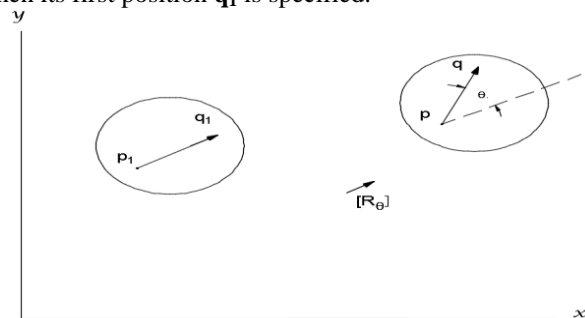


Fig. 4: Plane rigid body displacement.

Solving (2) for \mathbf{q} , we obtain

$$\mathbf{q} = [R_\theta](\mathbf{q}_1 - \mathbf{p}_1) + \mathbf{p} \quad (3)$$

Equations (2) and (3) are in a convenient form for carrying out algebraic manipulations for plane motion the rotation matrix is 2×2 matrix.

$$\begin{bmatrix} \mathbf{q} \\ 1 \end{bmatrix} = [D] \begin{bmatrix} \mathbf{q}_1 \\ 1 \end{bmatrix} \quad (4)$$

The 3×3 matrix $[D]$ is the plane displacement matrix. The displacement matrix equation has advantages in repetitive numerical calculations where all matrix elements are defined in terms of the specified displacement of the reference point \mathbf{p} and the angular displacement of the rigid body. The displacement matrix for pose description is shown in the following equations

$$[D_{1j}] \begin{bmatrix} p_{1x} & q_{1x} & r_{1x} \\ p_{1y} & q_{1y} & p_{1y} \\ 1 & 1 & 1 \end{bmatrix} = \begin{bmatrix} p_{jx} & q_{jx} & r_{jx} \\ p_{jy} & q_{jy} & p_{jy} \\ 1 & 1 & 1 \end{bmatrix} \quad (5)$$

from which

$$[D_{1j}] = \begin{bmatrix} p_{jx} & q_{jx} & r_{jx} \\ p_{jy} & q_{jy} & p_{jy} \\ 1 & 1 & 1 \end{bmatrix} \begin{bmatrix} p_{1x} & q_{1x} & r_{1x} \\ p_{1y} & q_{1y} & p_{1y} \\ 1 & 1 & 1 \end{bmatrix}^{-1} \quad (6)$$

Note that a constant z , coordinate = 1 has been specified for all points.



B. Constant Length Constraint

In contrast to kinematic analysis—where mechanism dimensions are known and the resulting mechanism output parameters are calculated—in kinematic synthesis, mechanism output parameters are known and the corresponding mechanism dimensions are calculated. The specified positions are known as precision points, and the synthesized mechanism will be expected to guide the rigid body such that the position error is zero at the precision points. It is sometimes convenient to describe rigid body motion in terms of the known displacement of specified points fixed in the rigid body. For example, the displacement of a plane rigid body could be specified completely by the displacement of three arbitrary non collinear points **p**, **q**, and **r** fixed in the body.

Assume that a two-joint link (i.e., a crank) is capable of guiding a plane rigid body from position 1 through a series of three positions. A point **a** on the guided body must pass through a sequence of positions, all of which are the same distance from a point **a₀** on the fixed reference member. Each of the links must satisfy a condition of constant length, where points **a_j**=(*a_{jx}*, *a_{jy}*), **a₀**=(*a_{0x}*, *a_{0y}*) are representative of a typical guiding links **aa₀**, **b_j**=(*b_{jx}*, *b_{jy}*) and **b₀**=(*b_{0x}*, *b_{0y}*) are representative of a typical guiding links **bb₀**. These constraint equations become

$$(\mathbf{a}_j - \mathbf{a}_0)^T (\mathbf{a}_j - \mathbf{a}_0) = (\mathbf{a}_1 - \mathbf{a}_0)^T (\mathbf{a}_1 - \mathbf{a}_0) \tag{7}$$

$$(\mathbf{b}_j - \mathbf{b}_0)^T (\mathbf{b}_j - \mathbf{b}_0) = (\mathbf{b}_1 - \mathbf{b}_0)^T (\mathbf{b}_1 - \mathbf{b}_0) \tag{8}$$

Where

$$\mathbf{a}_j = [D_{1j}] \mathbf{a}_1 \text{ and } j=2,3,\dots n$$

$$\mathbf{b}_j = [D_{1j}] \mathbf{b}_1$$

Constant length for the crank is *L₁* and for the follower is *L₂*. Therefore (7) and (8) can be written as

$$([D_{1j}] \mathbf{a}_1 - \mathbf{a}_0)^T ([D_{1j}] \mathbf{a}_1 - \mathbf{a}_0) - L_1^2 = 0 \tag{9}$$

$$([D_{1j}] \mathbf{b}_1 - \mathbf{b}_0)^T ([D_{1j}] \mathbf{b}_1 - \mathbf{b}_0) - L_2^2 = 0 \tag{10}$$

C. Design Variables

The required movement/rotation of links in this work can be employed in stamping, clamping or welding operations, the double-crank Grashof's criterion [24] is applied to the link lengths constraints which is *L+S < A+B* (for rotation) where *L*, *S*, *A* and *B* represents lengths of longest link, shortest link, and other two links respectively. Therefore, in the present case Grashof's equation should be incorporated in the optimization algorithm and should be satisfied. Another feature that should be incorporated to ascertain the functionality of the proposed work is the transmission angle (*μ*) which should be between 50° and 135°. Also the clearance for the stamping should exceed 1 cm.

III. MOTION GENERATION NON-LINEAR OPTIMIZATION GOAL PROGRAM

Formulating Eqns. (9) and (10) into a single objective function that accommodates an indefinite number of *N* sets of

prescribed motion generation parameters to be minimized yields

$$f(\mathbf{X}) = \sum_{i=1}^N \left\{ \left[([D_{1i}] \mathbf{a}_1 - \mathbf{a}_0)^T ([D_{1i}] \mathbf{a}_1 - \mathbf{a}_0) - L_1^2 \right]^2 + \left[([D_{1i}] \mathbf{b}_1 - \mathbf{b}_0)^T ([D_{1i}] \mathbf{b}_1 - \mathbf{b}_0) - L_2^2 \right]^2 \right\} \tag{11}$$

where $\mathbf{X} = (a_{0x}, a_{0y}, a_{1x}, a_{1y}, L_1, b_{0x}, b_{0y}, b_{1x}, b_{1y}, L_2)^T$.

Equation (11) and design variables (i.e. Grashof's case and transmission angle) constitute a goal program from which mechanism solutions that approximate the prescribed rigid-body motion points and satisfy the design variables are calculated.

The algorithm employed for solving this goal program (a nonlinear constraints problem) is SQP (Sequential Quadratic Programming) which uses Quasi-Newton approach to solve its QP (Quadratic Programming) subproblem and line search approach to determine iteration step. The merit function used by [25] and [26] is used in the following form:

$$\Psi(\mathbf{X}) = f(\mathbf{X}) + \sum_{k=1}^m r_k \max[0, g_k(\mathbf{X})] \tag{12}$$

where *g_k*(**X**) represents each inequality constraint, *m* is the total number of inequality constraints and the inequality constraint penalty parameter is

$$(r_{l+1})_k = \max \left\{ \lambda_k, \frac{1}{2} \left((r_l)_k + \lambda_k \right) \right\}. \tag{13}$$

In Eqn. (13) *λ_k* are estimates of the Lagrange multipliers and *l* is the iteration index for calculating the penalty parameter *r_k* for each inequality constraint (*l*=0, 1, 2, 3, ...).

After specifying initial guesses for the unknown variables in the goal program (**X**), the following SQP steps were employed to calculate the unknown variables:

1. calculate *λ_k* and *(r_{l+1})_k*, (where *l*=0 and *k*=1...*m*)
2. solve Eqn. (12) using Quasi-Newton method
3. calculate *(r_{l+1})_k* using Eqn. (13) (where *l*=*l*+1 and *k*=1...*m*)
4. repeat step 2 with newly-calculated *r_k*

Steps 2 through 4 constitute a loop that is repeated until the penalty term in Eqn. (12), $\sum_{k=1}^m r_k \max[0, g_k(\mathbf{X})]$, is less than a specified penalty term residual *ε*. The reader should refer to [25] and [26] regarding the calculation of the Lagrange multipliers and initial penalty parameters in step 1.

IV. EXAMPLE

Now, all coordinates for the five poses are shown in the prescribed values in SI units (cm) in Table I, motion generation program can be programed with prescribed values; let us calculate *a_{0y}*, *L₁* and *a_{1x}* and *a_{1y}* given an initial guesses as **a₀** = (0,0), **a₁**=(1, 1), **b₀**=(0, 0.5) and **b₁**=(1.5, 1.5). Initial guesses are needed for Newton Raphson technique to solve the line search method through sequential quadratic programming, this is also done by [27], where the author concluded that the synthesis is greatly affected by the quality of initial guess.



Inverse Kinematic Synthesis of Motion Generation Four-bar Stamping Mechanism

Table I: Prescribed Value for Coupler Points **p**, **q** and **r** for 5 Poses

	p	q	r
Pose 1	-0.7651, 2.5077	0.3493, 2.7456	1.1830, 2.1679
Pose 2	-1.1234, 2.3743	-0.0234, 2.6719	0.8402, 2.1400
Pose 3	-1.4499, 2.1871	-0.3642, 2.5331	0.5221, 2.0400
Pose 4	-1.7367, 1.9517	-0.6642, 2.3368	0.2394, 1.8761
Pose 5	-1.9760, 1.6752	-0.9150, 2.0909	0.0014, 1.6562

Using the motion generation goal program in (11), the fixed and moving pivot locus points calculated from the non-linear optimization problem. After incorporating the fixed and moving pivot loci into the updated motion generator selection algorithm with a transmission angle (trans.) condition of $50^\circ \leq \mu \leq 120^\circ$, and a Grashof's condition of 'double-crank, the fixed and moving pivot coordinates of the selected planar four-bar motion generator for press mechanism (Fig. 5) are $\mathbf{a}_0 = (0, -0.0348)$, $\mathbf{a}_1 = (-0.5229, 1.8890)$, $\mathbf{b}_0 = (1, 0.5061)$ and $\mathbf{b}_1 = (1.0008, 2.0072)$, and For $\mathbf{b}_0 - \mathbf{b}_1$ (follower length), $(L_2) = 1.5011$. This mechanism has crank, coupler, follower, and ground link lengths of 1.9936, 1.5283, 1.5011, and 0.9657, respectively, (satisfying Grashof's crank-rocker conditions) and produces the transmission profile illustrated in Fig. 8. Coupler poses one through five correspond to crank angles of $\theta_1 = 133.5271^\circ, 112.8409^\circ, 92.5959^\circ, 72.2693^\circ, 8.6884^\circ$, respectively. The fixed and moving pivot locus points calculated from the non-linear optimization problem are illustrated in Fig. 5.

Table II: Rigid-Body Positions Achieved by Synthesized Motion Generator

	p	q	r
Pose 1	-0.7651, 2.5077	0.3493, 2.7456	1.1830, 2.1679
Pose 2	-1.1244, 2.3736	-0.0245, 2.6716	0.8393, 2.1399
Pose 3	-1.4513, 2.1860	-0.3657, 2.5324	0.5208, 2.0396
Pose 4	-1.7379, 1.9504	-0.6655, 2.3358	0.2382, 1.8754
Pose 5	-1.9768, 1.6739	-0.9159, 2.0899	0.0006, 1.6555

If the a_{0x} is given the range of $[0, 0.1, 0.2, \dots, 1]$, then the nonlinear optimization will give the loci curve for moving and fixed pivots as shown in Fig. 6. All four associated loci on the curves are solution by itself and mechanism can be extracted as shown in the solid line

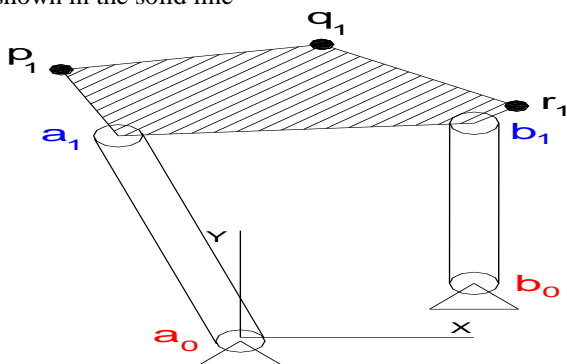


Fig.5: Synthesized four-bar mechanism

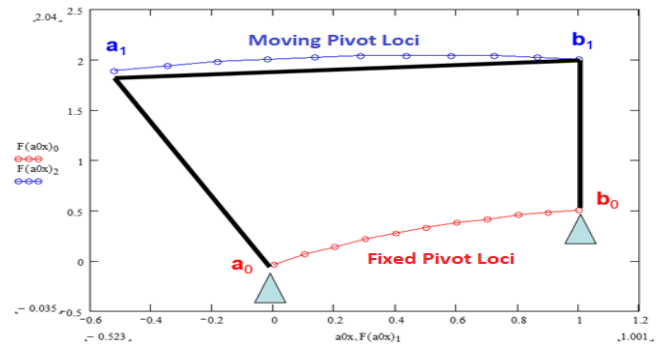


Fig. 6: Mechanism selected from calculated solution loci for fixed and moving pivots

The structural error can be calculated by comparing the prescribed poses of coupler points **p**, **q**, and **r** to the achieved poses as shown in Fig. 7. The results in this example is measured by the error between the prescribed **p**, **q**, and **r** as shown in Table I and the achieved **p**, **q**, and **r**, as shown in Table II. This error is shown in Fig. 7 which gives maximum value of 0.0018cm (0.018mm). that is in comparison consider to be small error which proves that this method has an advantage value over vector method for two reasons; one it is faster in computation than vector analysis and second because sometimes the motion is desired and need inverse kinematics to determine the mechanism coordinates. The final shape of the synthesized stamping machine is shown in Fig's 8(2D) and built in ADAMS Fig.9(3D) to extract the trace path of the ram, transmission angle and driving crank angle with positive x-axis Fig. 10. This robot hand can be used in stamping machine where the stamp can be fixed at the end effector and the motion will make the coupler to go from left to right as shown. This stamping machine can be used in high volume production line (e.g. water bottle expiration date) or just stamp one paper.

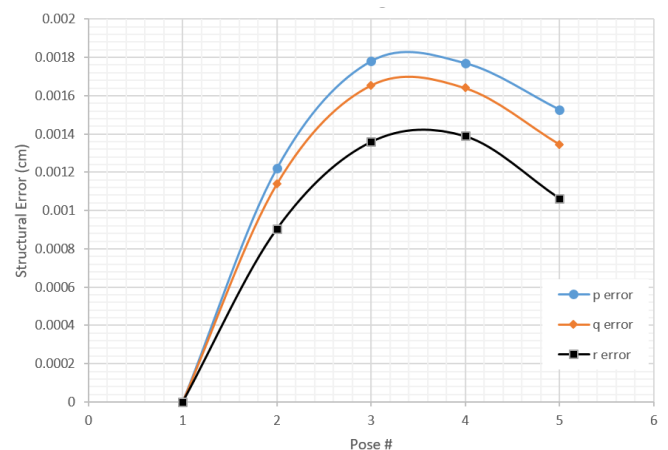


Fig. 7 Structural error of coupler points **p**, **q**, and **r** in five poses

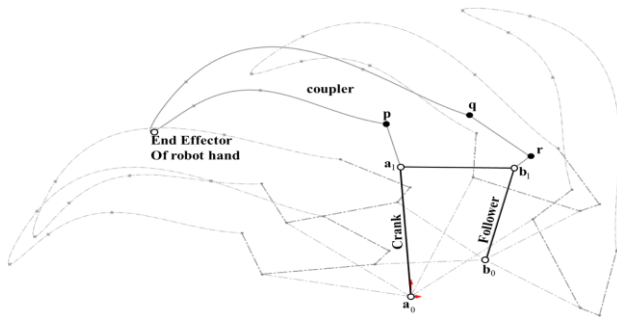


Fig. 8: Working envelope for the synthesized stamping mechanism

Figure 9 shows the crank angle (θ), transmission angle (μ) and BDC clearance (δ). BDC clearance (δ) as calculated by ADAMS is 2.9 cm which satisfies the design variable mentioned in Section II.C. The synthesized stamping mechanism also satisfies the condition of transmission angle (μ) which is $50^\circ \leq \mu \leq 135^\circ$ as shown in the shaded area in Fig. 10.

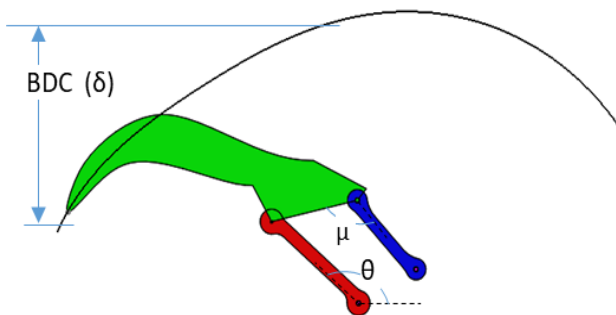


Fig. 9: ADAMS model for the synthesized stamping mechanism

The proportional relationship between the crank angle (θ) and transmission angle (μ) is shown in Fig. 10. The operational region (i.e. shaded area) shows the synthesized stamping mechanism, the outside area beyond the operational region shows the full extension of the path if this mechanism would move to the extreme conditions. The crank angle can start from 60° (CW) to 150° (CCW) where lockup mechanism occurs, this corresponds to transmission angle region of 80° to 146° , respectively.

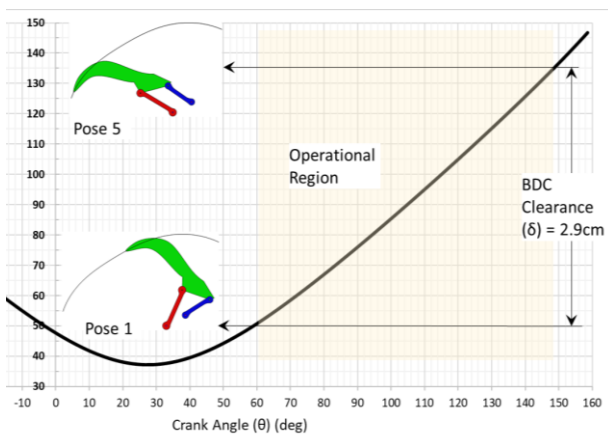


Fig. 10: ADAMS result shows relationship between the crank angle (θ) and transmission angle (μ). Crank angle below zero degree is cropped for clarity purpose. When the pivots a_1 , b_1 and b_0 are collinear. Such a state is possible when the four-bar mechanism reaches a “lock-up” or binding position.

V. CONCLUSION

Matrix inversion method and motion generation were used to synthesize four-bar stamping mechanism. The achieved mechanism motion passes through prescribed poses with very minimum error of 0.2% cm. A great deal of attention must be given to the location of coupler point and avoid to put them in one line with fixed ratio, this will result in displacement matrix to have ill condition and cannot be inverted. The mathematical model was programmed using MathCAD and mechanism layout and poses were extracted using CAD software. The synthesized mechanism was then inverted to ADAMS to extract all motion properties such as transmission angle, crank angle and the vertical distance of the stamping station (i.e. stroke to BDC). The proposed method can be used for any four bar application ranging from small mechanisms to heavy lifting mechanisms.

REFERENCES

1. Welding, “https://www.youtube.com/watch?v=AXRpo02JkAM.”
2. R. C. Hibbeler, “Engineering Mechanics Statics, 13th Edition,” Pearson Prentice Hall, Upper Saddle River, NJ, USA, p. 321, 2013.
3. F.-B. S. Mechanism, “https://nl.mathworks.com/matlabcentral/mlc-downloads/downloads/submissions/36536/versions/14/previews/Simscape_Multibody_Parts_Lib_R17b/Examples/Linkages/html/html/sm_links_5bar_stamp.htm?access_key=.”
4. E. Mechanism, “https://www.youtube.com/watch?v=PUzT8zdPWt8.”
5. S. Garm, “https://shyamgarg31.wordpress.com/2014/05/01/cad-models-stamping-mechanism/.”
6. S. Mechanism, “https://www.youtube.com/watch?v=CO0y3CY47Rc.”
7. R. Sehgal and A. Sharma, “A graphical approach for kinematic design and development of an automatic stamping machine using four bar chain,” *Indian J. Eng. Mater. Sci.*, vol. 15, no. 3, pp. 229–235, 2008.
8. O. Vinogradov, “FUNDAMENTALS of KINEMATICS and DYNAMICS of MACHINES and MECHANISMS,” CRC Press, LLC, pp. 3–4, 2000.
9. H. Sen Yan and W. R. Chen, “Variable input speed approach for improving the output motion characteristics of Watt-type presses,” *Int. J. Mach. Tools Manuf.*, vol. 40, no. 5, pp. 675–690, 2000.
10. J. Hu, Y. Sun, and Y. Cheng, “High mechanical advantage design of six-bar Stephenson mechanism for servo mechanical presses,” *Adv. Mech. Eng.*, vol. 8, no. 7, pp. 1–12, 2016.
11. Y. Luo and R. Du, “Procedia Engineering An Investigation on the Impact Noise of a Six-Bar Linkage Mechanical Press,” vol. 29, pp. 1486–1491, 2012.
12. H. Li and Y. Zhang, “Seven-bar mechanical press with hybrid-driven mechanism for deep drawing: Part 1: kinematics analysis and optimum design,” *J. Mech. Sci. Technol.*, vol. 24, no. 11, pp. 2153–2160, 2010.
13. M. E. Kütük and L. C. Dülger, “Hybrid Seven-bar Press Mechanism,” *Teh. Glas.*, vol. 12, no. 3, pp. 181–187, 2018.
14. P. L. Tso and K. C. Liang, “A nine-bar linkage for mechanical forming presses,” vol. 42, no. March 2001, pp. 139–145, 2002.
15. A. Hernandez, O. Altuzarra, V. Petuya, C. Pinto, and E. Amezcua, “A robot for non-destructive testing weld inspection of offshore mooring chains,” no. June, pp. 1–12, 2018.
16. S. Park et al., “Optimal design of toggle-linkage mechanism for clamping applications,” *Mech. Mach. Theory*, vol. 120, pp. 203–212, 2018.
17. S. A. Bhojne, “Computer Aided Kinematic Analysis of Toggle Clamping Mechanism,” *IOSR J. Mech. Civ. Eng.*, vol. 01, no. 01, pp. 49–56, 2016.
18. Y. Wu and X. Zhou, “Simulation Research of Five-Bar Pneumatic Clamping Mechanism,” *Appl. Mech. Mater.*, vol. 456, pp. 28–31, 2013.

19. A. Prabhakaran and A. Ghosal, *Machines, Mechanism and Robotics*, no. October 2018. Springer Singapore, 2019.
20. K. A. I. He, Y. Luo, C. T. O. M. Kong, and R. Du, "Trajectory Planning , Optimization and Control of a Hybrid Mechanical Press," no. June 2016, 2009.
21. K. J. Kyriakopoulos and G. N. Saridis, "Minimum jerk path generation," pp. 364–369, 2003.
22. A. Piazzi and A. Visioli, "Global Minimum-Jerk Trajectory Planning of Robot Manipulators," vol. 47, no. 1, pp. 140–149, 2000.
23. C. W. S. C.H. and Radcliffe, "Kinematics & Mechanisms Design," *Kinematics & Mechanisms Design*. John Wiley&Sons, 1978.
24. K. J. Waldron and G. L. Kinzel, *Kinematics, dynamics, and design of machinery*. John Wiley & Sons, Singapore, 2003.
25. S. P. Han, "A globally convergent method for nonlinear programming," *J. Optim. Theory Appl.*, vol. 22, no. 3, pp. 297–309, 1977.
26. M. J. D. Powell, "a Fast Algorithm for Nonlinearly Constrained," *Numer. ana-lysis, Lect. notes Math. (Ed. G. A. Watson)*, (Springer-Verlag, Berlin, Ger.), vol. 630, 1976.
27. R. R. Bulatović and S. R. Dordević, "On the optimum synthesis of a four-bar linkage using differential evolution and method of variable controlled deviations," *Mech. Mach. Theory*, vol. 44, no. 1, pp. 235–246, 2009.

AUTHORS PROFILE



Bilal M Oraik is an MSc student in the Faculty of Informatics and Computing, University Sultan Zainal Abidin, Besut Campus, 22200 Besut, Terengganu, Malaysia. He received his BSc. In Mathematics from Irbid National University in the year of 2002; since then he worked as a math teacher in Jordan and Saudi Arabia.



Nurnadiyah Zamri Nurnadiyah Zamri received the PhD Degree from Universiti Malaysia Terengganu, Malaysia in 2015. She is a senior lecturer in the Faculty of Informatics and Computing, Universiti Sultan Zainal Abidin, Malaysia. Her research of interest include fuzzy decision making, fuzzy expert system and cloud computing. She has published more than 40 journal papers, proceeding papers and book of chapter.



Yahia M. Al-Smadi is an Assistant Professor of Mechanical Engineering at Jordan University of Science and Technology (JUST), Irbid-Jordan, He received his BSc. from JUST in Mechanical Engineering the year of 1999; MSc in Manufacturing Systems Engineering from New Jersey Institute of Technology (NJIT), NJ-USA in the year of 2002; and in 2009 he has obtained his PhD from NJIT in Mechanical Engineering. He over 15 years of industrial experience in the fields of Mechanism Synthesis, Structural Dynamics, and Biomechanics Simulation and Synthesis. He is an active member of various professional bodies like JEA, ASME, HMS, ASE, and AGMA. He has published 3 book chapters, journal papers and international conference papers in the fields of nonlinear dynamics, finite element analysis, robotics, simulation and mechanism synthesis. He is also a reviewer for a dozen of international peer review journals in mechanical engineering.